EEET ECOLOGICAL ENGINEERING & ENVIRONMENTAL TECHNOLOGY

Ecological Engineering & Environmental Technology 2024, 25(2), 281–291
https://doi.org/10.12912/27197050/176706
ISSN 2719–7050, License CC-BY 4.0

Received: 2023.11.17
Accepted: 2023.12.19
Published: 2024.01.01

Cleaning and Management of Water Contaminated with Pesticides through the Process of Adsorption in the Natural Clay of Brari

Esad Behrami[1], Isak Berbatovci[2*], Kledi Xhaxhiu[3], Nensi Isak[3], Adelaida Andoni[3], Arianit Reka[4], Xhuljeta Hamiti[3], Zehra Hajrulai Musliu[5], Risto Uzunov[5]

[1] Departament of Chemistry, Faculty of Natural and Mathematics Sciences, University of Prishtina, Kosova
[2] Departament of Health Managment, Alma Matter Europaea, Campus College" Rezonanca", Kosova
[3] Faculty of Natural Sciences, Department of Chemistry, University of Tirana, Tirana, Albania
[4] Faculty of Natural Sciences and Mathematics, University of Tetovo, Tetovo, Republic of North Macedonia
[5] Faculty of Veterinary, Medicine Cyril and Methodius University in Skopje, Republic of North Macedonia
* Corresponding author's email: isakberbatovci1@gmail.com

ABSTRACT

This study aimed to investigate the potential for widespread application of clay in the purification of water polluted with pesticides and water management through the absorption and desorption of dimethoate and methomyl in the natural clay of Brari (Tirana). While the maximum adsorption of methomyl on Brari clay was reached in 12 hours, the maximum adsorption of dimethoate on Brari clay was reached in 48 hours. To compare the adsorption of methomyl and dimethoate on Brari clay, their water degradation time was also taken into account. Dimethoate dissolves quickly; a contact period of 1–2 hours is sufficient to desorb 81.2% of the material. Dimethoate dissolves in water at 25 °C and has a half-life $t_{1/2}$ = 30 days. Methomyl is desorbed even faster; in just two hours, 96.2% of the material is desorbed. At 25 °C, dimethoate has a half-life of $t_{1/2}$ = 14 days and a high solubility of 58 g/L in water. Because methomyl and dimethoate bind poorly to clay, they can contaminate surface and groundwater.

Keywords: methomyl, dimethoate, clay, management, adsorption, desorption.

INTRODUCTION

Understanding common materials like clays is essential to comprehending global biological, environmental, and sedimentary processes. They are useful for a variety of purposes due to their chemical and physical characteristics. They are commonly found in fine-grained rocks and soil. Clays have been employed in numerous applications since prehistoric times, including the chemical industry, building materials, health, environment, and civil engineering (Moreno-Maroto and Alonso-Azcárate 2018, Ural 2018). Due to the detrimental effects of wastewater on the environment and ecosystem after discharge, wastewater treatment is a major global concern. This has caused a number of treatment procedures to be looked into for their efficacy on a worldwide scale (Khan et al. 2022). The past has seen the proposal of multiple guidelines for environmental risk assessment by various agencies (ANSES, 2011; EC, 2003; EMA, 2006; US EPA, 1992a, US EPA, 1996, US EPA, 2011a). Therefore, consideration should be given to the risk assessment of effluent wastewater releases from wastewater treatment plants (WWTP) (Khan et al. 2021). Because clay minerals contain high concentrations of SiO_2 and Al_2O_3, they are categorized as hydrated alumino-silicates. In particular, kaolin clays are mostly made of SiO_2, Al_2O_3, and water and have a chemical composition of $Al_2Si_2O_5(OH)_4$ or Al_2O_3 and $2SiO_2$ and $2H_2O$ (Schackow et al. 2020, Rouabhia et al. 2018). The majority of samples are composed of SiO_2 and Al_2O_3, but NC clay is unique in that it contains significantly more Fe_2O_3

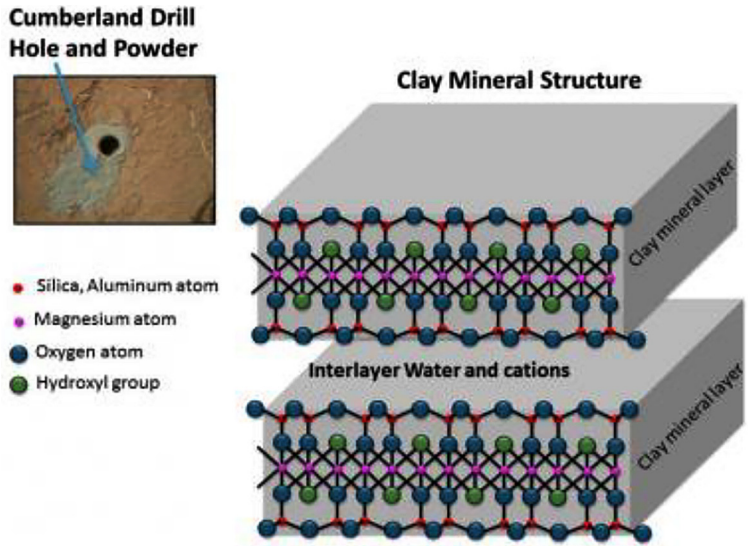

Figure 1. Clay structure

(approximately 28%) and less Al_2O_3 (17%) than other samples (Reches et al. 2018).

The influence of the main structure-forming oxides SiO_2/Al_2O_3 and H_2O/Al_2O_3 on the physical, rheological and colloidal-chemical properties of lithium-containing aluminosilicate suspensions Al_2O_3-nSiO_2-mH_2O in the system are presented for the first time (Guzii et al. 2021).

Analysis of particle sizes reveals that WC has the highest clay content (91.88%) and NC has the lowest (49.88%) (Fig. 1). The best way to characterize natural clays is to examine their crystallite compositions. In this study, the particle size distribution was defined not by the grain size obtained through comminution, but rather according to the natural crystallite size of the minerals found in the clays (Jongs et al. 2018).

The nutrients in the soil dissolve and produce positively or ions with a negative charge. Anions are the positively charged type of ion. Ions can also be classified as negatively charged. The nutrients that exist as cations are Ca^{2+}, Mg^{2+}, NH_4^+, K^+, H^+, Na^+, Al^{3+}, Fe^{2+}, Mn^{2+}, Zn^{2+}, and Cu^{2+}. Among the nutrients that exist as anions are Cl^-, NO_3^-, SO_4^{2-}, $H_2PO_4^-$, HPO_4^{2-}, BO_3^{3-}, and MoO_4^{2-} (Efretuei et al. 2016).

The cation exchange capacity of the soil is measured (CEC), a chemical property. Cations can be retained and stored in the soil. Lower in the soil profile, negatively charged soil particles attract and hold on to cations, or positively charged ions, preventing them from eroding. Exchangeable cations are the cations that remain in soil particles (Khaledian et al. 2017). Conversely, anions, or negatively charged ions, are repelled by negatively charged soil particles. Efretuei et al. (2016) suggest that this indicates negatively charged nutrients, like nitrates, sulfate, and chlorides, are prone to seeping down the soil profile.

Pesticides are often applied carelessly, which exacerbates the issue of soil accumulation (Tudi et al. 2021). Several variables, including soil microflora and properties, influence the fate of applied pesticides. As a result, the pesticides go through several adsorption/desorption, transport, and degradation processes (Behrami et al. 2022).

Moreover, it has been noted that pesticides affect the mineralization of soil organic matter, a crucial soil characteristic that establishes the quality and productivity of soil. For example, a significant

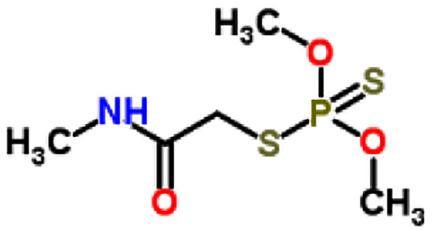

Figure 2. Structure of dimethoate $C_5H_{12}NO_3PS_2$ (Guleria et al. 2011, Sipes et al. 2013)

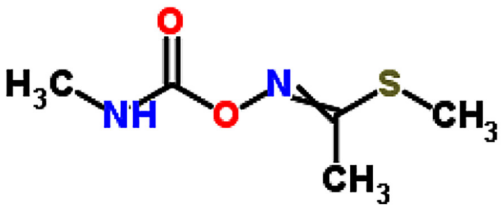

Figure 3. Structure of methomyl $C_5H_{10}N_2O_2S$ (Manavi et al. 2024)

drop in soil organic matter was noted after the application of four herbicides (atrazine, primeextra, paraquat, and glyphosate) (Sebiomo et al. 2010).

MATERIALS AND METHODS

Materials

This study was made possible by the FSHN-Univeristy of Tirana and FBV-Univeristy of Prishtina, the Kosovo Agricultural Institute, the FV Agency, and the Faculty of Mathematical Sciences-Natural, University of Tetovo (FMNS-UT). The clay samples were collected in the vicinity of Tirana, Albania, or Brari. After chopping and sieving the clay, the 1.5 μm portion was chosen for further study. The separated portion was preserved in plastic bottles with a hermetically sealed lid after being dried at 150 °C for four hours. Following a series of tests, the working methodology could be confirmed and ultimately the final methodological scheme was obtained, as presented below: Dichloromethane and ethyl acetate were combined (1:3, vw) to create the extraction solvent, and this ratio worked extremely well to extract methomyl and dimethoate from their aqueous solutions. In each case, 3 milliliters of extractant solvent were used to carry out the extraction of ethyl acetate and dimethoate. As an internal standard, dibutyl phthalate (DBF) was added to an aqueous solution at the start of the extraction process. However, because of its planar structure, DBF adsorbed from clay along with dimethoate and ethyl acetate, changing the adsorption results. DBF was added to prevent adsorption competition with dimethoate and methomyl; however, even in these instances, notable variations in the obtained results have been observed. When the internal standard DBF was added to the organic extract that had been separated from the aqueous solution of dimethoate and methomyl, the best results were eventually obtained. During the extraction process, sodium chloride (NaCl) has been employed as an anti-emulsifier to prevent the formation of emulsions. Using analytical standards of DBF (99.5%), methomyl (99%), and dimethoate (96%), measurements were conducted using the GC/MS method until the ideal operating parameters were obtained. The initial results of the study indicate that between two and twenty-four hours, there was no appreciable adsorption from the dimethoate and methomyl aqueous solution. On this basis, the contact time was extended from 24 to 72. From the differences between the initial and final concentrations, the adsorbed and desorbed amounts (mg/g) of methomyl and dimethoate were calculated:

$$q = (C_0 - C_e) \times V/m \quad (1)$$

where: C_0 – the initial concentration of adsorbate (mg/L), C_e – the final concentration of adsorbate (mg/L), V – the volume of the solution (L), m – the mass of the adsorbent (clay material) (g).

After conducting several tests and making measurements using GC/MS, it was possible to identify the ideal gas chromatograph method conditions, which were maintained as standard conditions for the duration of the investigation. All the conducted research was aimed at studying the capacity of the natural clay of Brari and its application in the cleaning of waters polluted with pesticides and consequently their management.

Methods

Three methods were used in the conducted research. Finally, the clay was characterized by X-ray fluorescence (XRF) spectrometry and scanning electron microscope (SEM) VEGA3 LMU method. To quantitatively evaluate the clay of Brari, X-ray energy dispersion spectroscopy (INCA Energ 250 System Microanalysis System) was used, which was combined with the SEM method at VEGA3 LMU. The X-ray fluorescence spectrometer was model ARL 900 with ppm-100% measuring capacity, measuring accuracy + 0.10%, and a 40 kV – 80 mA X-ray tube. The SEN method detector had an accelerating voltage of 20 kV set. Finally, GCMS-QP2010S, ARL 9900, gas chromatography (GC) method with mass spectrometry (MS) capability was used. The carrier gas, helium, had a flow rate of 1.71 milliliters per minute. The temperature settings for the column were 277.1 °C for the working column, 290.1 °C for the detector and injector, and 214.7 kPa for the header pressure.

RESULTS

X-ray analysis of Brari clay

The X-ray fluorescence spectrometer data given in Table 1 show the composition of Brari

Table 1. Brari clay composition data

Type of clay	Fe	SiO_2	MgO	Al_2O_3	Ni	Co	CaO	Cr_2O_3
Brari	6.55	43.80	6.28	6.48	0.07	0.00	8.75	0.44

clay with a high content of SiO_2, Al_2O_3, and CaO. The highest content of these binary compounds is proportionally related to the montmorillonite content of the clay. This finding is in full accordance with the data published by (Xhaxhiu, Prifti, and Zitka 2020).

Elemental composition of Brari clay determined using the SEM-EDX method

The clay of Brari was analyzed with the SEM-EDX method to understand the topography and composition, below are the SEM-EDX results of the natural clay of Brari (Tirana). The SEM-analyzed images of Brari clay with a 100 µm resolution (spectrum 1) were shown in Figure 4, while Table 2 and Figure 5 presented the basic SEM-EDX analysis of Brari clay. This analysis reveals that Si (as SiO_2) predominates in the composition of Brari clay, followed by Al (as Al_2O_3). Figure 6 presents the images of Brari clay analyzed with a scanning electron microscope with a resolution of 100 µm (spectrum 2), while Figure 7 and Table 3 show the results of the elementary analysis of Brari clay with the SEM-EDX method, where its composition is confirmed again, so these data confirm the

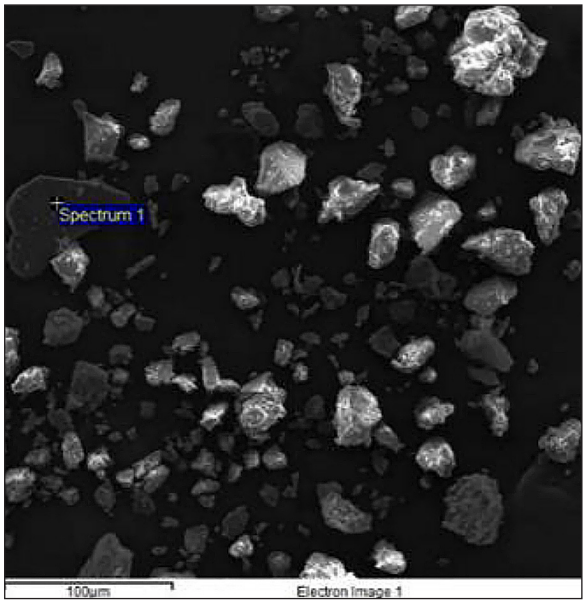

Figure 4. Brari clay images analyzed by scanning electron microscope

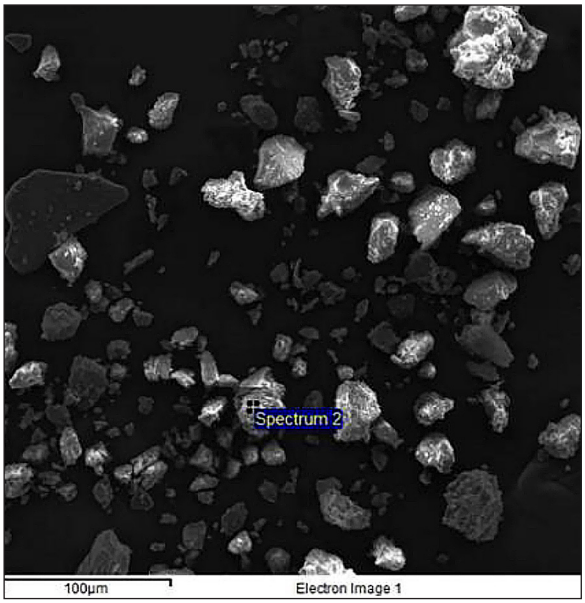

Figure 6. Brari clay images analyzed by scanning electron microscope with a resolution: of 100 µm (spectrum 2)

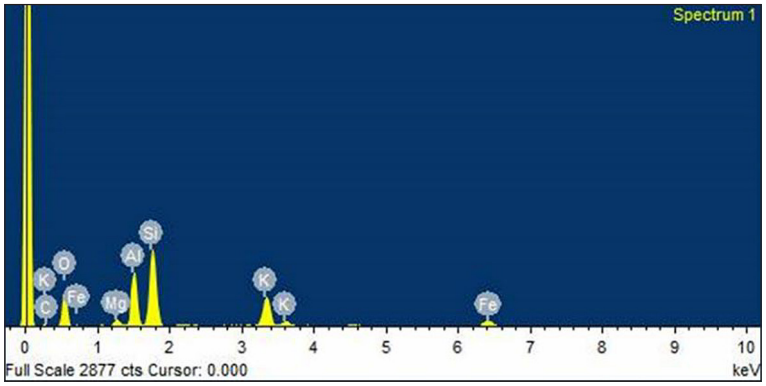

Figure 5. Representative spectrum of elementary-quantitative identification

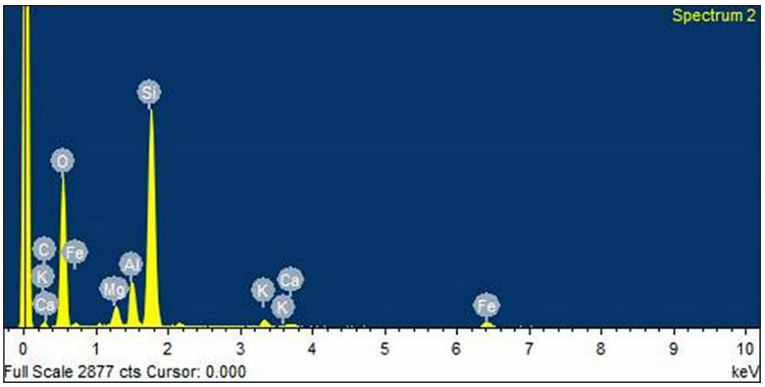

Figure 7. Representative spectrum of elementary-quantitative identification

Table 2. Elementary analysis and quantitative content information

Element	% by weight	% atomic
C K	2.67	4.51
O K	52.16	66.24
Mg K	1.36	1.14
Al K	11.16	8.40
Si K	17.55	12.69
K K	9.75	5.07
Fe K	5.35	1.95
Total	100.00	

Table 3. Elementary analysis and quantitative content information

Element	% by the weight	% of the element
C K	13.45	19.09
O K	62.86	66.99
Mg K	1.79	1.25
Al K	3.16	2.00
Si K	15.89	9.64
K K	0.80	0.35
Ca K	0.35	0.15
Fe K	1.70	0.52
Total	100.00	

dominance of the element Si in the form SiO_2, followed by Al in the form Al_2O_3.

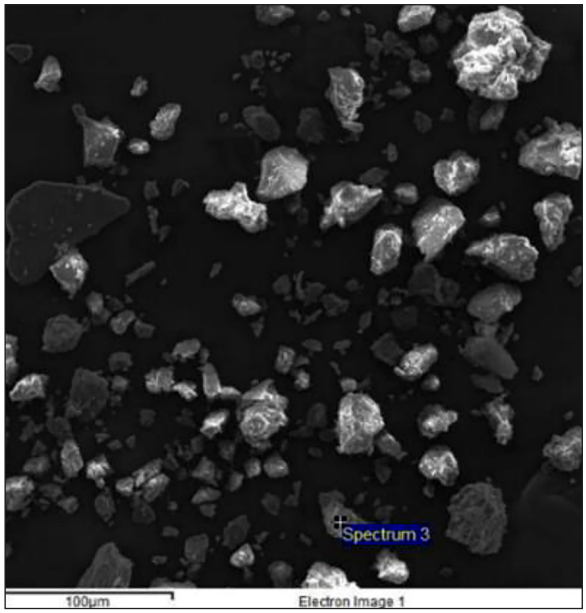

Figure 8. Brari clay images analyzed by using scanning electron microscope with a resolution: of 100 µm (spectrum 3)

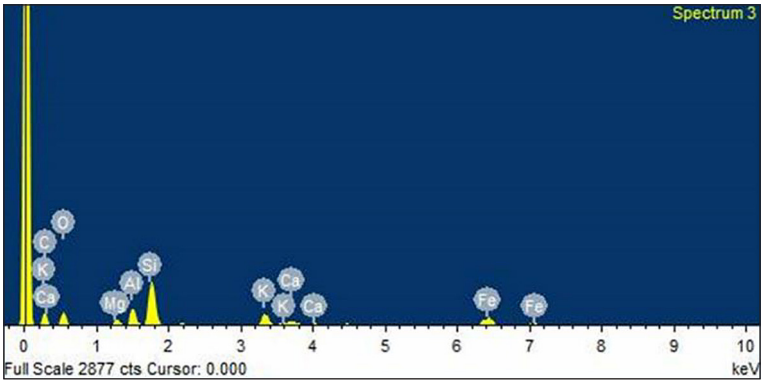

Figure 9. Representative spectrum of elementary-quantitative identification of Brari clay, which has a resolution of 100 µm (spectrum 3)

A third scan with a resolution of 100 μm was also carried out, the results of which are presented in Figure 8, which shows the images of Brari clay analyzed with a scanning electron microscope (SEM) with a resolution of 100 μm (spectrum 3), while Figure 9 and Table 4, present the results of the elemental analysis of Brar clay with

Table 4. Elementary analysis and quantitative content information

Element	% by the weight	% of the element
C K	46.56	59.92
O K	30.91	29.86
Mg K	1.17	0.74
Al K	2.94	1.68
Si K	8.04	4.43
K K	3.17	1.25
Ca K	1.09	0.42
Fe K	6.11	1.69
Total	100.00	

Table 5. Elementary analysis and quantitative content information

Element	% by the weight	% of the element
C K	21.67	29.57
O K	58.71	60.16
Mg K	3.41	2.30
Al K	3.77	2.29
Si K	6.44	3.76
K K	1.25	0.52
Fe K	4.76	1.40
Total	100.00	

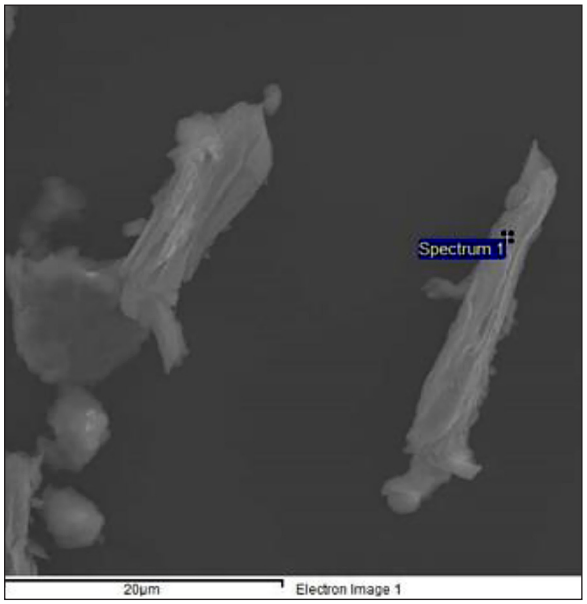

Figure 10. Brari clay images analyzed by scanning electron microscope with a resolution: of 20 μm (spectrum 1)

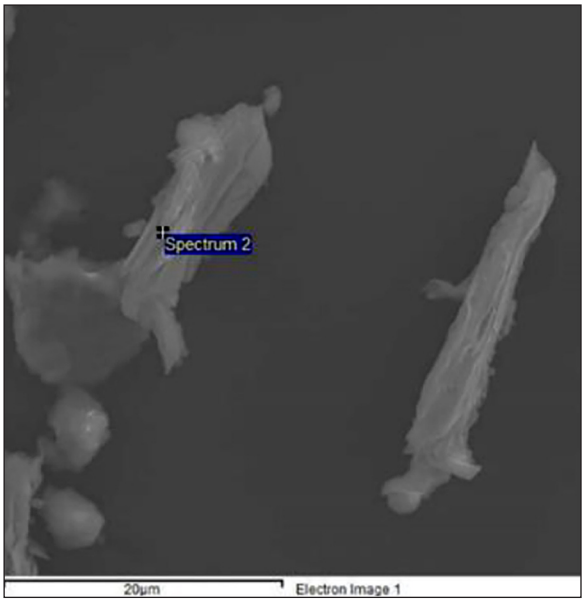

Figure 12. Brari clay images analyzed by scanning electron microscope with a resolution: of 20 μm (spectrum 2)

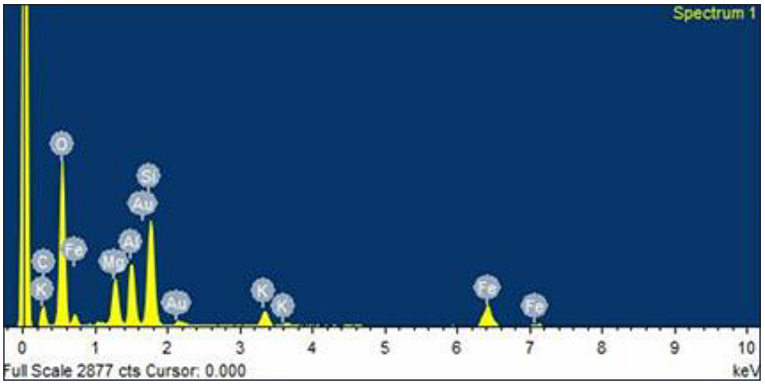

Figure 11. Representative spectrum of elementary-quantitative identification of Brari clay, which has a resolution of 20 μm (spectrum 1)

the SEM-EDX method, where its composition is confirmed again, so these data confirm the dominance of the element Si in the form of SiO_2, followed by Al in the form of Al_2O_3. From all three repeated measurements: spectrum 1; spectrum 2 and spectrum 3 with SEM-EDX with 100 μm resolution for Brari clay, the results that confirm the predominance of Si and Al in the form of SiO_2 and Al_2O_3 were obtained. The following are the SEM-EDX measurements with a resolution of 20

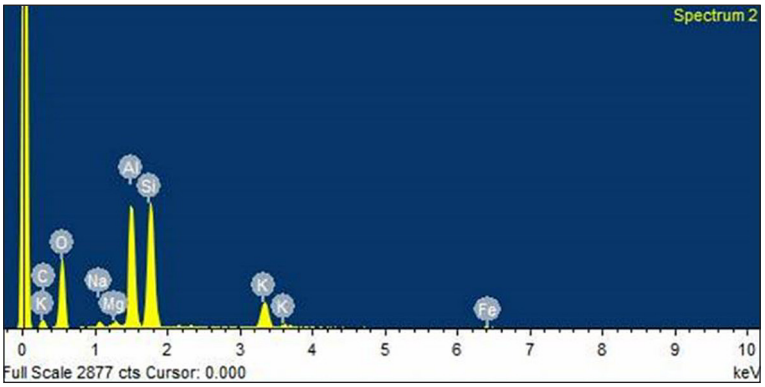

Figure 13. Representative spectrum of elementary-quantitative identification of Brari clay, which has a resolution of 20 μm (spectrum 2)

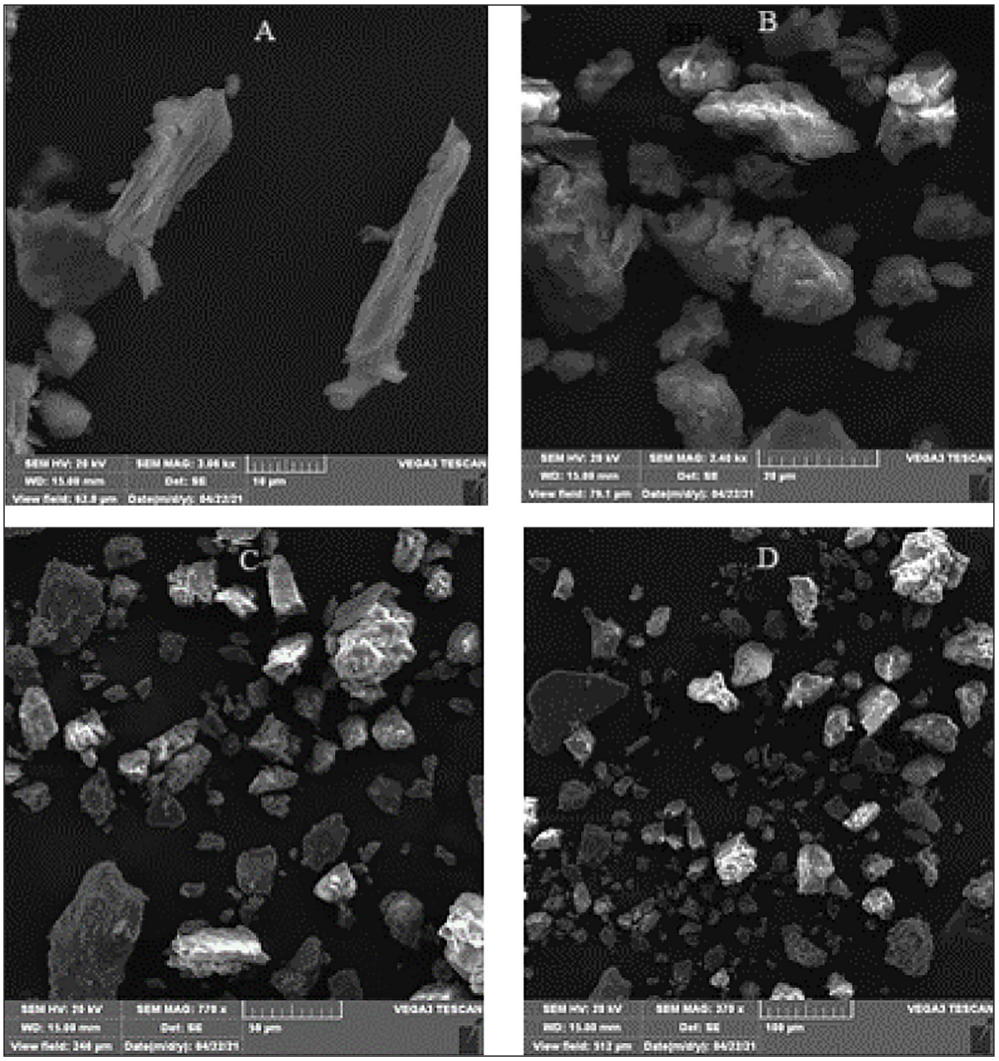

Figure 14. Brari clay images analyzed by scanning electron microscope with resolution: 10 μm, 20 μm, 50 μm, and 100 μm

Table 6. Elementary analysis and quantitative content information

Element	% by the weight	% of the element
C K	21.53	30.33
O K	50.01	52.89
Na K	0.68	0.50
Mg K	0.47	0.33
Al K	10.90	6.83
Si K	12.24	7.38
K K	3.69	1.60
Fe K	0.49	0.15
Total	100.00	

µm for Brari clay (spectrum 1). SEM-EDX measurements with a resolution of 20 µm, which are presented in Figures 10, 11, 12, and 13 (spectrum 1 and spectrum 2) as well as Tables 5 and 6 (spectrum 1 and spectrum 2) confirm the assertion that in Brari clay the elements As in the form of SiO_2 and Al in the form of Alumina (Al_2O_3).

SEM images with results are presented below 10, 20, 50, and 100 µm of Brari clay. Figure 14 (A, B, C, D) compares the clay images. As it can be seen from the images with a resolution of 100 µm, 50 µm, 20 µm, and 10 µm, Brari clay consists of particles whose shape is elongated (branch). Previous studies on this clay (Behrami and Avdiu 2023) showed that Brari clay has a significant specific surface area and is considered a good absorbent.

GC/MS analysis of Brari clay

Adsorption of dimethoate and methomyl in Brari clay – the analyses were performed with a gas chromatography-mass spectrometer. The results obtained from the adsorption process of dimethoate and methomyl with an initial concentration of 25 mg/l in natural Brari clay are presented

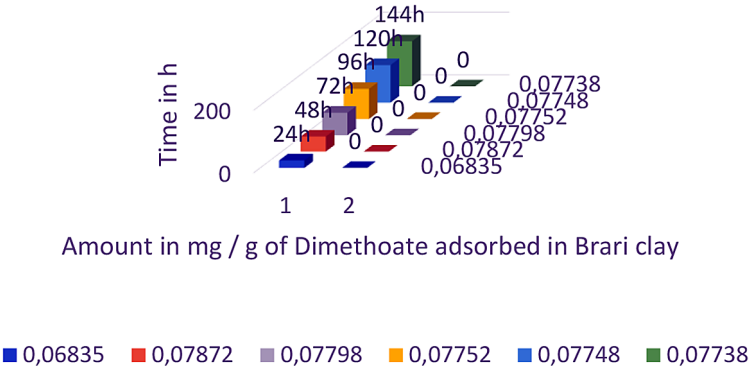

Figure 15. Adsorption of dimethoate in Brari clay

Table 7. Amount adsorbed of dimethoate

Nr. probation	Time in h	Adsorbed amount mg/5g	Adsorbed amount mg/g	KR (%)
1	24	0.34175	0.06835	34.1
2	48	0.3936	0.07872	21.6
3	72	0.3899	0.07798	19.7
4	96	0.3876	0.07752	20.5
5	120	0.3874	0.07748	10.9
6	144	0.3869	0.07738	8.5

Table 8. Amount adsorbed of methomyl

Nr. probation	Time in h	Adsorbed amount mg/5g	Adsorbed amount mg/g	KR (%)
1	12	0.182	0.0364	34.1
2	24	0.179	0.0358	21.6
3	48	0.177	0.0354	19.7
4	72	0.1745	0.0349	20.5
5	96	0.173	0.0346	10.9
6	120	0.167	0.0334	8.5

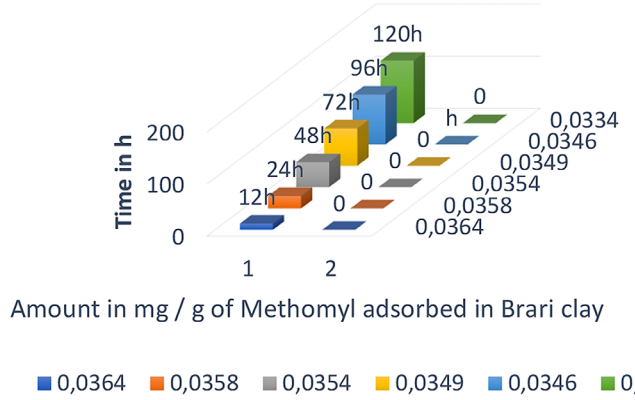

Figure 16. Adsorption of methomyl in Brari clay

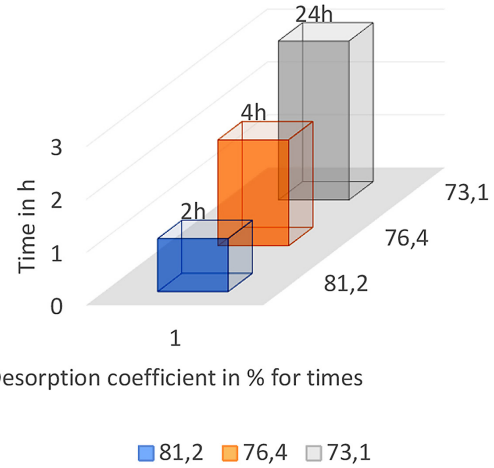

Figure 17. Desorption of dimethoate in Brari clay

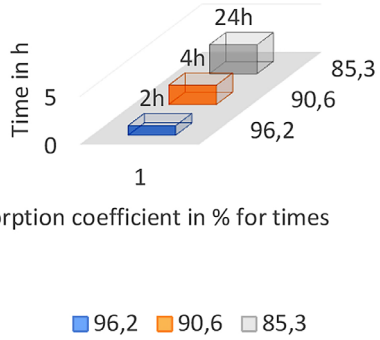

Figure 18. Desorption of methomyl in Brari clay

in Tables 7 and 8 as well as plotted in Figures 15 and 16. From the data of this group of experiments, it appears that Brari clay presents good adsorbent properties to dimethoate and methomyl. Studying the dependence of the adsorption of dimethoate and methomyl on Brari clay in aqueous solutions, from the time of clay + H_2O contact, it is noticed that from 2 h to 24 h there is no visible adsorption of dimethoate and methomyl on clay. Therefore further studies were extended to time intervals from 24 h to 144 h. Longer intervals are of no interest because the rates of spontaneous increase great hydrolysis of dimethoate and methomyl.

From the data presented in Table 7 and Figure 15, it can be seen that dimethoate as an organophosphorus insecticide is adsorbed on Brari clay in values from 0.06835 mg/g for 24 h to 0.07738 mg/g for 144 h. These findings enabled to conclude that the window of time between 24 and 48 hours is the most favorable for dimethoate adsorption on Brari clay. Also noteworthy is the nearly nonexistent amount of dimethoate that was adsorbed in Brari clay between the hours of two and twenty-four. For this reason, the data from the time 24 h to 144 h was presented. Table 8 and Figure 16 present the adsorption of methomyl in

Table 9. Desorption coefficient in % for times

Nr.	Type of clay	Desorption coefficient in % for times		
		2h	4 h	24 h
1	Brari	81.2	76.4	73.1

Table 10. Desorption coefficient in % for times

Nr.	Type of clay	Desorption coefficient in % for times		
		2 h	4 h	24 h
1	Brari	96.2	90.6	85.3

Brari Clay from which it can be seen that methomyl is adsorbed less compared to dimethoate. Thus, the amount adsorbed in mg/g of methomyl in Brari clay ranges from 0.0364 mg/g for 12 h and drops to 0.0334 after 120 h. Hence, it may be inferred that methomyl has the optimal time to be adsorbed in Brari clay up to 12 h, after this time there is a linear decrease in the amount adsorbed. Future studies should focus on Methomyl adsorption at time intervals from 2 h to 12 h.

The series 2 presented in Figures 15 and 16 is a comparative series with the series 1, which shows that for zero time the adsorption would be zero. The percentage progress of the desorption process of dimethoate from Brari clay is shown in Table 9 and Figure 17. From the obtained data, it was noticed that dimethoate is desorbed 81.2% in the first two hours, while over time the desorbed % decreases. It is worth mentioning that after 24 h the desorption process decreases and a moment comes when this process returns to adsorption. The progress of desorption process was also shown in the percentage of methomyl from Brari clay in Table 10 and Figure 18. From the obtained data, the same phenomenon can be observed and it is seen that methomyl in the first two hours is desorbed 96.2% while over time the desorbed % decreases and falls to 85.3%.

CONCLUSIONS

All images analyzed by using SEM of Brari clay show that the composition of Brari clay is dominated by Si (as SiO_2), followed by Al (as Al_2O_3). Adsorption of dimethoate and methomyl in Brari natural clay were performed by using the method of gas chromatography with mass spectrometer (GC-MS). From the data of this set of experiments, it appears that the clay of Brari presents good absorbent properties to dimethoate and methomyl. By studying the dependence of the adsorption of dimethoate and methomyl from Brar clay in aqueous solutions, from the moment of clay + H_2O contact, it is observed that in the time interval from 2 h to 24 h there is no visible adsorption of dimethoate and methomyl in the clay. Therefore, further studies were extended to the time interval from 24 h to 144 h. Longer intervals are not of interest, due to spontaneous hydrolysis of dimethoate and methomyl increases. For a contact period of one to two hours, both pesticides underwent a rapid desorption process. The use of natural clay Brari for the purification of water polluted by pesticides represents a good practical opportunity. In all the experiments, it was found that the clay of Brari has great adsorbing potential for pesticides and it is recommended to be used massively for the purification of polluted waters.

REFERENCES

1. Behrami E. and Avdiu V. 2023. The process and kinetics of pesticide desorption from clay as a function of cleaning polluted waters. *Processes* 11 (4): 1180. https://doi.org/10.3390/pr11041180.
2. Behrami E., Xhaxhiu K., Dragusha B., Reka A., Andoni A., Hamiti X., and Drushku S. 2022. The removal of atrazine and benalaxyl by the fly ash released from Kosovo a power plant. *International Journal of Analytical Chemistry* 2022 (January): 9945199. https://doi.org/10.1155/2022/9945199.
3. Efretuei A., Gooding M., White E., Spink J., and Hackett R. 2016. Effect of nitrogen fertilizer timing on nitrogen use efficiency and grain yield of winter wheat in Ireland. *Irish Journal of Agricultural and Food Research* 55 (June). https://doi.org/10.1515/ijafr-2016-0006.
4. Guleria S., Singh B. and Shanker A. 2011. Distribution behaviour of dimethoate in tea leaf. *Journal of Environmental Protection* 2 (April). https://doi.org/10.4236/jep.2011.24056.
5. Guzii S.G., Kurska T., Andronov V., and Adamenko M. 2021. Influence of basic oxides ratio Li_2O/Al_2O_3, SiO_2/Al_2O_3 and H_2O/Al_2O_3 on physical, rheological and colloidal-chemical properties of lithium containing alumosilicate suspensions in the system xLi_2O-Al_2O_3-$nSiO_2$-mH_2O. *Materials Science Forum* 1038: 193–202. https://doi.org/10.4028/www.scientific.net/MSF.1038.193.
6. Jongs L.S., Jock A.A., Ekanem O.E. and Jauro A. 2018. Investigating the industrial potentials of some selected nigerian clay deposits. *Journal of Minerals and Materials Characterization and Engineering* 6(6): 569–86. https://doi.org/10.4236/jmmce.2018.66041.
7. Khaledian Y., Brevik E., Pereira P., Cerdà A., Fattah M., and Tazikeh H. 2017. Modeling soil cation exchange capacity in multiple countries. *Catena* 158 (July): 194–200. https://doi.org/10.1016/j.catena.2017.07.002.
8. Khan A.H., Aziz H.A., Khan N.A., Dhingra A., Ahmed S. and Naushad M. 2021. Effect of seasonal variation on the occurrences of high-risk pharmaceutical in drain-laden surface water: A risk analysis of Yamuna River. *Science of the Total Environment* 794 (Nov): 148484. https://doi.org/10.1016/j.scitotenv.2021.148484.

9. Khan N.A., Bokhari A., Mubashir M., Klemeš J.J., El Morabet R., Khan R.A., Alsubih M., et al. 2022. Treatment of hospital wastewater with submerged aerobic fixed film reactor coupled with tube-settler. *Chemosphere* 286 (January): 131838. https://doi.org/10.1016/j.chemosphere.2021.131838.
10. Manavi M.A., Nasab M.H.F. and Baeeri M. 2024. Methomyl. In: *Encyclopedia of Toxicology (Fourth Edition)*, edited by Philip J. Wexler, 197–204. Oxford: Academic Press. https://doi.org/10.1016/B978-0-12-824315-2.00451-6.
11. Moreno-Maroto J.M. and Alonso-Azcárate J..2018. What is clay? A new definition of 'clay' based on plasticity and its impact on the most widespread soil classification systems. *Applied Clay Science* 161 (September): 57–63. https://doi.org/10.1016/j.clay.2018.04.011.
12. Reches Y., Thomson K., Helbing M., Kosson D., and Sanchez F. 2018. Agglomeration and reactivity of nanoparticles of SiO_2, TiO_2, $Al2O_3$, Fe_2O_3, and clays in cement pastes and effects on compressive strength at ambient and elevated temperatures. *Construction and Building Materials* 167 (April): 860–73. https://doi.org/10.1016/j.conbuildmat.2018.02.032.
13. Rouabhia F., Nemamcha A. and Moumeni H. 2018. Elaboration and characterization of mullite-anorthite-albite porous ceramics prepared from algerian kaolin. *Cerâmica* 64 (369): 126–32. https://doi.org/10.1590/0366-69132018643692297.
14. Schackow A., Correia S.L., and Effting C. 2020. Influence of microstructural and morphological properties of raw natural clays on the reactivity of clay brick wastes in a cementitious blend matrix. *Cerâmica* 66 (May): 154–63. https://doi.org/10.1590/0366-69132020663782852.
15. Sebiomo A., Ogundero V., and Bankole S. 2010. Effect of four herbicides on microbial population, soil organic matter and dehydrogenase activity. *African Journal of Biotechnology* 10 (September): 770–778.
16. Sipes N.S., Martin M.T., Kothiya P., Reif D.M., Judson R.S., Richard A.M., Houck K.A., Dix D.J., Kavlock R.J., and Knudsen T.B. 2013. Profiling 976 toxcast chemicals across 331 enzymatic and receptor signaling assays. *Chemical Research in Toxicology* 26 (6): 878–895. https://doi.org/10.1021/tx400021f.
17. Tudi M., Ruan H.D., Wang L., Lyu J., Sadler R., Connell D., Chu C., and Phung D.T. 2021. Agriculture development, pesticide application and its impact on the environment. *International Journal of Environmental Research and Public Health* 18 (3). https://doi.org/10.3390/ijerph18031112.